LS FFT-based Channel Estimators Using Pilot-Embedded Data-Bearing Approach in Space-Frequency Coded MIMO-OFDM Systems

Chaiyod Pirak†*, Z. Jane Wang‡, K. J. Ray Liu†, Somchai Jitapunkul*
†Department of Electrical & Computer Engineering, University of Maryland, College Park, USA.
‡Department of Electrical & Computer Engineering, University of British Columbia, Vancouver, Canada
*Department of Electrical Engineering, Chulalongkorn University, Bangkok, Thailand
Email: chaiyod.p@gmail.com, zjanew@ece.ubc.ca, kjrliu@eng.umd.edu, somchai.j@chula.ac.th

***Abstract*— Multiple-input multiple-output (MIMO) orthogonal frequency division multiplexing (OFDM) is one prominent communication system for realizing high speed data transmission services. One critical issue for such systems is channel estimation. In this paper, we first develop a pilot-embedded data-bearing (PEDB) approach for joint channel estimation and data detection. Then we propose a least square (LS) FFT-based channel estimator by employing the concept of FFT-based channel estimation to improve the performance of the PEDB-LS channel estimation. Also, the effects of model mismatch error when considering non-integer multipath delay profiles, and its performance are investigated. We further propose an adaptive LS FFT-based channel estimator that employs the optimum number of significant taps. Simulation results reveal that the adaptive LS FFT-based estimator provides superior performance under quasi-static channels or low Doppler's shift regimes.**

I. Introduction

Recently, multiple-input multiple-output (MIMO) orthogonal frequency division multiplexing (OFDM) systems have been proposed for increasing the communication capacity as well as the reliability of the wireless communication systems by exploiting the transmitter and receiver diversities [1]. However, these systems need an accurate channel state information (CSI) for coherently decoding the transmitted data, e.g. a maximum-likelihood (ML) decoder. Hence, channel estimation is of critical importance.

Various channel estimation schemes have been recently proposed for MIMO-OFDM systems [2]-[4]. In [4], the FFT-based channel estimation using a certain number of significant taps for estimating the channel impulse response in a temporal domain was proposed. Despite the efficient computational complexity of this scheme, it could suffer from an error floor caused by a non-integer multipath delay spread in the wireless channels, known as a *model mismatch error*. The model mismatch error, or the leakage effect, was first mentioned in single-input single-output (SISO)-OFDM systems employing the FFT-based channel estimation [5]. Without the knowledge of channel correlation information, two methods could be used to reduce the leakage effect: 1) by changing the exponential basis functions in the FFT-based approach to the polynomial basis functions [6], and 2) by employing a proper number of significant taps to construct a channel frequency response in the FFT-based approach [4]. In the former, although the approach [6] provides better performance than the FFT-based approach [4] under the non-integer multipath delay profiles, its performance is worse under the integer multipath delay profiles. Furthermore, this approach imposes higher computational complexity than that of the FFT-based approach, and a general rule of designing the optimum window length is not fully discovered. Given the efficient implementation and reliability, the FFT-based approach is still attractive. However, the optimal solution of choosing the number of significant taps remains unsolved. Here we plan to find the optimal criteria for obtaining the optimum number of significant taps when the knowledge of channel correlation information or Doppler's shift is not available. The main contributions of this paper are:

- We develop and analyze the performances of pilot-embedded data-bearing (PEDB) least-square (LS) and LS FFT-based channel estimators for MIMO-OFDM systems.
- We study the relationship between the mean-squared error (MSE) and the model mismatch error of the LS FFT-based channel estimator for determining the optimum number of significant taps, and hence, propose an adaptive LS FFT-based channel estimation approach.

The organization of this paper is as follows. In section II, we briefly introduce the wireless channel and system models used in this paper. In section III, we propose the pilot-embedded data-bearing approach for joint channel estimation and data detection. Under this pilot-embedding framework, in section IV, we propose the LS FFT-based channel estimator and study the performance analysis for the PEDB-LS and LS FFT-based channel estimation approaches. In section V, we propose the adaptive LS FFT-based channel estimation. In section VI, the performance of the proposed schemes are examined via simulations, and the conclusion is given in section VII.

II. Wireless Channel and System Models

We consider a $K-$tone SF-coded OFDM system with L_r receive and L_t transmit antennas. The complex baseband impulse response of the wireless channel between the a^{th} receive antenna and the b^{th} transmit antenna can be described by [4]

[1]This work was partially supported by a Ph.D. scholarship from Commission on Higher Education, Ministry of Education, Thai Government and a grant from the Cooperation Project between Department of Electrical Engineering and Private Sector for Research and Development, Chulalongkorn University, Thailand.

1-4244-0270-0/06/$20.00 (c)2006 IEEE

This full text paper was peer reviewed at the direction of IEEE Communications Society subject matter experts for publication in the WCNC 2006 proceedings.

$$h_{ab}(t,\tau) = \sum_l \gamma_l(t)\delta(\tau - D_l), \quad (1)$$

where D_l is the delay of the l^{th} path and $\gamma_l(t)$ represents the corresponding complex amplitude. $\gamma_l(t)$'s are modelled as wide-sense stationary (WSS), narrowband complex Gaussian processes, which are independent for different paths. We assume that all the signals transmitted from different transmit antennas to the receive antennas undergo independent fading, and the channel average power is normalized to have $\sum_l \sigma_l^2 = 1$ with σ_l^2 being an average power of the l^{th} path. For OFDM systems with tolerable leakage, the normalized frequency response of the OFDM systems at the k^{th} $(k = 0, \ldots, (K-1))$ subcarrier between the a^{th} receiver and the b^{th} transmitter can be described by [4]

$$H_{ab}(m,n,k) = \sum_{l=0}^{L-1} h_{ab}(m,n,l) F_K^{k\tau_l}, \quad (2)$$

where $h_{ab}(m,n,l) \triangleq h_{ab}(m, nT_f, \tau_l t_s)$, $F_K = \exp(-j2\pi/K)$, $t_s = 1/(K\Delta f)$, with Δf being the tone spacing, is the sample interval of the system, T_f is the OFDM block length, and m denotes the index of a group of N-OFDM blocks described next. L is the number of nonzero paths, and τ_l $(l = 0, \ldots, L-1)$ is the l^{th} path's delay sampled at rate t_s, e.g. $D_l = \tau_l t_s$. The average power of $h_{ab}(m,n,l)$ and the value of L depend on the delay profile and the dispersion of the wireless channels. For simplicity, we omit the time index n in all notations in the next text.

At the transmitter side, the MPSK-data symbols are coded by the space-frequency (SF) block code, e.g. [1], and grouped to construct the $L_t \times KN$ SF-coded data matrix $\mathbf{S}(m)$, where N denotes the number of OFDM blocks, and m denotes the N-OFDM-block index. In our proposed pilot-embedded data-bearing approach, the SF-coded data matrix $\mathbf{S}(m)$ is embedded by the pilot signal, so we have the SF-coded symbol matrix with size $L_t \times KM$, where M denotes the number of OFDM blocks included in one SF-coded symbol block. To eliminate the intersymbol interference (ISI), a cyclic prefix is employed with the length of cyclic extension being no smaller than τ_{L-1}. In this paper, we consider quasi-static frequency-selective Rayleigh fading channels, meaning that the channel remains constant over the SF-coded symbol block but changes in a block-by-block basis. By assuming tolerable power leakage and perfect time/frequency synchronization, the received signal of the m^{th} SF-coded symbol block can be described by

$$\mathbf{Y}(m) = \mathbf{H}(m)\mathbf{U}(m) + \mathbf{Z}(m), \quad (3)$$

where $\mathbf{Y}(m)$ is a $L_r \times KM$ matrix; $\mathbf{H}(m)$ is the $L_r \times KL_t$ channel matrix in which the a^{th} row of $\mathbf{H}(m)$ is $[\mathbf{H}_{a1}(m), \ldots, \mathbf{H}_{aL_t}(m)]$ where $\mathbf{H}_{ab}(m) = [H_{ab}(m,0), \ldots, H_{ab}(m,K-1)]$; $\mathbf{Z}(m)$ is the $L_r \times KM$ additive white Gaussian noise (AWGN) matrix with zero mean and variance $\frac{\sigma^2}{2}\mathbf{I}_{(L_r KM \times L_r KM)}$ per real dimension; and $\mathbf{U}(m)$ is the $KL_t \times KM$ equivalent SF-coded symbol matrix. Throughout this paper, we assume that the channels and noise, and channels from different paths are mutually uncorrelated.

III. Pilot-Embedded Data-Bearing Approach

In this section, we first present the main ideas of the pilot-embedded data-bearing approach. We then briefly introduce the PEDB-LS channel estimation and PEDB-ML data detection.

A. Pilot-Embedded Data-Bearing Approach

In the pilot-embedded data-bearing approach for joint channel estimation and data detection, the equivalent SF-coded symbol matrix $\mathbf{U}(m)$ can be described as follows,

$$\mathbf{U}(m) = \mathbf{D}(m)\mathbf{B} + \mathbf{C}, \quad (4)$$

where $\mathbf{D}(m)$ denotes the $KL_t \times KN$ equivalent SF-coded data matrix constructed from the matrix $\mathbf{S}(m)$ using the $K \times K$ matrix-diagonalized operator $\text{diag}\{\cdot\}$, where the $((b-1)K+1)^{th}$ row to the $(bK)^{th}$ row of $\mathbf{D}(m)$ are $[\text{diag}\{[\mathbf{S}(m)]_{b,1:K}\}, \ldots, \text{diag}\{[\mathbf{S}(m)]_{b,(N-1)K+1:NK}\}]$ with $x:y$ denotes the column/row index interval ranging x to y; $\mathbf{B}$ is the $KN \times KM$ data bearer matrix; and $\mathbf{C}$ is the $KL_t \times KM$ pilot matrix. Notice that the K diagonal elements of a $(b,c)^{th}$ submatrix, $c = 1, \ldots, M$, represented in $\mathbf{U}(m)$ by the $((b-1)K+1)^{th}$ row to the $(bK)^{th}$ row and the $((c-1)K+1)^{th}$ column to the $(cK)^{th}$ column are the c^{th} transmitted SF-coded OFDM block at the b^{th} transmitter in the m^{th} SF-coded symbol block-group. In addition, the energy constraint $\mathrm{E}[\|\mathbf{D}(m)\|^2] = KL_t$ is maintained for the equivalent SF-coded data matrix. Substituting (4) into (3), we have the received signal matrix as

$$\mathbf{Y}(m) = \mathbf{H}(m)(\mathbf{D}(m)\mathbf{B} + \mathbf{C}) + \mathbf{Z}(m). \quad (5)$$

Now, by the pilot-embedded data-bearing approach, the data bearer matrix $\mathbf{B}$ and the pilot matrix $\mathbf{C}$ are required to satisfy the following properties:

$$\mathbf{B}\mathbf{C}^T = \mathbf{0}_{(KN \times KL_t)},\ \mathbf{C}\mathbf{C}^T = \alpha\mathbf{I}_{(KL_t \times KL_t)}, \quad (6)$$

$$\mathbf{C}\mathbf{B}^T = \mathbf{0}_{(KL_t \times KN)},\ \text{and}\ \mathbf{B}\mathbf{B}^T = \beta\mathbf{I}_{(KN \times KN)}, \quad (7)$$

where β is the real-valued data-power factor and α is the real-valued pilot-power factor. The similar property $\mathbf{C}\mathbf{C}^T = \alpha\mathbf{I}$ in (6) is also suggested in [2] that it is the optimal criterion for the optimal training design for MIMO-OFDM systems. There are several possible structures of data-bearing and pilot matrices, in which the elements of these matrices are real numbers, that satisfy the properties (6) and (7). We are particularly interested in the case of Code-Multiplexing (CM)-Based Matrices, since it provides the superior performance among the three structures studied in [7].

We now describe the CM-Based matrices. The structures of these matrices are given as

$$\mathbf{B} = \sqrt{\beta}\text{WH}[1:N]_{(N \times M)} \otimes \mathbf{I}_{(K \times K)}, M = N + L_t,$$
$$\mathbf{C} = \sqrt{\alpha}\text{WH}[N+1:M]_{(L_t \times M)} \otimes \mathbf{I}_{(K \times K)}, \quad (8)$$

where $\text{WH}[x:y]$ denotes a sub-matrix created by splitting the $M \times M$ normalized Walsh-Hadamard matrix [8] starting from x^{th}-row to y^{th}-row and $\otimes$ denotes the Kronecker product. This structure provides an instructive example of the proposed general idea in (4) for pilot-embedding.

Notice that, in (8), the proposed scheme is a block-training scheme in which L_t OFDM blocks are used for estimating the CSI. As suggested in [3], [4], when using only one OFDM block for training in the MIMO-OFDM systems, the LS channel estimator for $\mathbf{H}_{ab}(m)$ exists only if $K \geq L_t L$. In general,

This full text paper was peer reviewed at the direction of IEEE Communications Society subject matter experts for publication in the WCNC 2006 proceedings.

in the case that $K < L_t L$ and $L \leq K$, the use of L_t OFDM blocks for training can guarantee the existence of the LS channel estimator and other better channel estimators, such as the LMMSE channel estimator [3].

B. Pilot-Embedded Data-Bearing LS Channel Estimation

We first extract the pilot part from the received signal matrix $\mathbf{Y}(m)$. By using the null-space and orthogonality properties in (6), respectively, we are able to extract the pilot part by simply post multiplying $\mathbf{Y}(m)$ in (5) by $\mathbf{C}^T$, and then dividing by α, to arrive at

$$\frac{\mathbf{Y}(m)\mathbf{C}^T}{\alpha} = \mathbf{H}(m) + \frac{\mathbf{Z}(m)\mathbf{C}^T}{\alpha}. \quad (9)$$

Let $\mathbf{Y}_1(m) = \frac{\mathbf{Y}(m)\mathbf{C}^T}{\alpha}$ and $\mathbf{Z}_1(m) = \frac{\mathbf{Z}(m)\mathbf{C}^T}{\alpha}$, we have

$$\mathbf{Y}_1(m) = \mathbf{H}(m) + \mathbf{Z}_1(m). \quad (10)$$

The PEDB-LS channel estimator can be obtained by minimizing the following mean-squared-error objective function,

$$\hat{\mathbf{H}}_{LS}(m) = \min_{\mathbf{H}(m)} \|\mathbf{Y}_1(m) - \mathbf{H}(m)\|^2. \quad (11)$$

It is straightforward to show that

$$\hat{\mathbf{H}}_{LS}(m) = \mathbf{Y}_1(m) = \frac{\mathbf{Y}(m)\mathbf{C}^T}{\alpha}. \quad (12)$$

C. Pilot-Embedded Data-Bearing ML Data Detection

We now describe the procedure of PEDB-ML data detection. First, we extract the data part from the received signal matrix $\mathbf{Y}(m)$. Using the null-space and orthogonality properties in (7), respectively, we are able to extract the data part by simply post multiplying $\mathbf{Y}(m)$ in (5) by $\mathbf{B}^T$, and then dividing by β,

$$\frac{\mathbf{Y}(m)\mathbf{B}^T}{\beta} = \mathbf{H}(m)\mathbf{D}(m) + \frac{\mathbf{Z}(m)\mathbf{B}^T}{\beta}. \quad (13)$$

Let $\mathbf{Y}_2(m) = \frac{\mathbf{Y}(m)\mathbf{B}^T}{\beta}$ and $\mathbf{Z}_2(m) = \frac{\mathbf{Z}(m)\mathbf{B}^T}{\beta}$, we have

$$\mathbf{Y}_2(m) = \mathbf{H}(m)\mathbf{D}(m) + \mathbf{Z}_2(m). \quad (14)$$

From the orthogonality of $\mathbf{B}$ in (7), we note that $\sum_{j'=1}^{KM} |B_{i',j'}|^2 = \beta, \ \forall i'$. Therefore, the data-bearer-projected noise $\mathbf{Z}_2(m)$ is AWGN with zero-mean and variance $\frac{\sigma^2}{2\beta}\mathbf{I}_{(KL_rN \times KL_rN)}$ per real dimension. Due to the i.i.d white Gaussian distribution of $\mathbf{Z}_2(m)$, the PEDB-ML receiver jointly decides the codewords for the d^{th} OFDM block in the m^{th} SF-coded data block by solving the following minimization problem,

$$\hat{\mathbf{D}}_{i,j}(m) = \min_{\mathbf{D}_{i,j}} \|\mathbf{Y}_{2_{s,j}}(m) - \hat{\mathbf{H}}_{s,i}(m)\mathbf{D}_{i,j}(m)\|^2,$$
$$i = 1 : KL_t, \ j = (d-1)K + 1 : dK,$$
$$s = 1 : L_r, \text{ and } d = 1, \ldots, N, \quad (15)$$

where $\hat{\mathbf{H}}(m)$ is the estimated channel matrix, e.g. $\hat{\mathbf{H}}(m) = \hat{\mathbf{H}}_{LS}(m)$. The codeword transmitted from the b^{th} transmitter is represented by $\hat{\mathbf{D}}_{i_b,j}(m)$, with $i_b = (b-1)K + 1 : bK$.

IV. The LS FFT-Based Channel Estimation and Performance Analysis

As shown in (9), the PEDB-LS channel estimate contains the channel frequency response that is contaminated by AWGN. In this section, we improve the performance of the PEDB-LS channel estimator by employing the basic concepts of the FFT-based approach proposed in [4].

A. LS FFT-Based Channel Estimation Approach

As suggested in [4], the FFT-based channel estimation approach first calculates the temporal LS channel estimate by using L significant taps, i.e. L's largest $\sum_{b=1}^{L_t} |\hat{H}_{LS_{ab}}(m,k)|^2$. The resulting temporal LS channel estimate is then FFT transformed to obtain the K-subcarrier channel frequency response.

Now let us propose the LS FFT-based channel estimator in details. From (12), we have $\hat{\mathbf{H}}_{LS_{ab}}(m) = ([\hat{\mathbf{H}}_{LS}(m)]_{a,(b-1)K+1:bK})^T$. From the channel model in (2), $\hat{\mathbf{H}}_{LS_{ab}}(m)$ can be expressed as

$$\hat{\mathbf{H}}_{LS_{ab}}(m) = \mathbf{F}\mathbf{h}_{ab}(m) + \mathbf{Z}_{1_{ab}}(m), \quad (16)$$

where $\mathbf{F}$ is the $K \times L$ matrix whose element $[\mathbf{F}]_{xy}$ is defined by $\exp[(-j2\pi/K)(x-1)\tau_y], \ x = 1, \ldots, K, \ y = 0, \ldots, L-1$; $\mathbf{h}_{ab}(m) = [h_{ab}(m,0), \ldots, h_{ab}(m, L-1)]^T$; and $\mathbf{Z}_{1_{ab}}(m) = ([\mathbf{Z}_1(m)]_{a,(b-1)K+1:bK})^T$.

Transforming the PEDB-LS channel estimate in (16) to the temporal PEDB-LS channel estimate by using the $K \times K$ IFFT matrix $\mathbf{G}$, whose element $[\mathbf{G}]_{xy}$ is defined by $\frac{1}{K}\exp(j2\pi/K)(x-1)(y-1), \ x, y = 1, \ldots, K$, we have

$$\hat{\mathbf{h}}_{LS_{ab}}(m) = \mathbf{G}\hat{\mathbf{H}}_{LS_{ab}}(m) = \mathbf{G}\mathbf{F}\mathbf{h}_{ab}(m) + \mathbf{G}\mathbf{Z}_{1_{ab}}(m). \quad (17)$$

Let $\mathbf{Z}^G_{1_{ab}}(m) = \mathbf{G}\mathbf{Z}_{1_{ab}}(m)$, it can be shown that

$$\hat{\mathbf{h}}_{LS_{ab}}(m) = [g(1), \ldots, g(K)]^T, \quad (18)$$

where $g(x) = \frac{1}{K}\sum_{l=0}^{L-1} h_{ab}(m,l) f(x-1-\tau_l) e^{j\xi(x-1-\tau_l)} + Z^G_{1_{ab}}(m,x)$ with $Z^G_{1_{ab}}(m,x)$ being the x^{th} element of $\mathbf{Z}^G_{1_{ab}}(m)$, $f(q) = \frac{\sin(\pi q)}{\sin(\pi q/K)}$ is the leakage function, and $\xi = \frac{(K-1)\pi}{K}$.

Obviously, from (18), if τ_l is an integer number, then the l^{th} element of the L largest elements of $\hat{\mathbf{h}}_{LS_{ab}}(m)$ is equal to $h_{ab}(m,l) + Z^G_{1_{ab}}(m,l)$, and the rest elements, which are not a member of the L largest elements, are equal to $Z^G_{1_{ab}}(m,e), \ e \neq l, \ e \in \{0, \ldots, K-1\} \backslash \mathcal{W}_1$ with $\mathcal{W}_1$ being the set of the L largest elements. As a result, by choosing L largest taps and replacing the $(K-L)$ remaining taps by zero is sufficient and optimal, resulting in the LS FFT-based estimate of the temporal channel impulse response $\hat{\mathbf{h}}_{FFT_{ab}}(m)$, since we completely capture the channel impulse response $\mathbf{h}_{ab}(m)$, and remove the excessive noise in the $(K-L)$ remaining taps. However, in reality, the l^{th} multipath delay τ_l is often a non-integer number, hence, the L-multipath channel impulse response dissipates to all K taps of $\hat{\mathbf{h}}_{LS_{ab}}(m)$ and thus results in the *model mismatch error*, which increases the channel estimation error, primarily caused by the AWGN $\mathbf{Z}^G_{1_{ab}}(m)$. This additional channel estimation error causes the severe error floor in the MSE of the channel estimation, and the detection error probability. Once the L (or P) largest taps are chosen and the rest taps are replaced by zero, the LS FFT-based estimated channel frequency response is determined by

$$\hat{\mathbf{H}}_{FFT_{a,b}}(m) = K\mathbf{G}^H\hat{\mathbf{h}}_{FFT_{ab}}(m). \quad (19)$$

B. Channel Estimation Error Performance Analysis

We now analyze the performance of the PEDB-LS and LS FFT-based channel estimators by using the MSE of channel estimation as the performance measure.

This full text paper was peer reviewed at the direction of IEEE Communications Society subject matter experts for publication in the WCNC 2006 proceedings.

1) PEDB-LS Channel Estimator: For arbitrary multipath delay profiles, the temporal channel impulse response between the a^{th} receiver and b^{th} transmitter can be described by,

$$\mathbf{h}_{ab}^{G}(m) = \mathbf{GF}\mathbf{h}_{ab}(m). \tag{20}$$

The channel estimation error can be readily described by

$$\tilde{\mathbf{h}}_{LS_{ab}}(m) = \mathbf{h}_{ab}^{G}(m) - \hat{\mathbf{h}}_{LS_{ab}} = -\mathbf{Z}_{1_{ab}}^{G}(m), \tag{21}$$

by referring to $\hat{\mathbf{h}}_{LS_{ab}}(m)$ in (17), and $\mathbf{h}_{ab}^{G}(m)$ in (20). Using (21), the $\mathrm{MSE}_{LS}(a,b)$ of the channel estimation is expressed as

$$\mathrm{E}[\|\tilde{\mathbf{h}}_{LS_{ab}}(m)\|^2] = \mathrm{E}[\| - \mathbf{Z}_{1_{ab}}^{G}(m)\|^2] = \frac{\sigma^2}{\alpha}, \tag{22}$$

by using $\mathrm{E}[|Z_{1_{ab}}^{G}(m,x)|^2] = \frac{\sigma^2}{K\alpha},\ x = 1,\ldots,K$, as referring to section III.B. It is worth noticing that (22) is also the MSE of the K-tap FFT-based channel estimation.

For L_r-receiver L_t-transmitter MIMO systems, the overall MSE_{LS} in (22) can be expressed as follows,

$$\mathrm{MSE}_{LS}^{T} = \sum_{a=1}^{L_t}\sum_{b=1}^{L_r}\mathrm{MSE}_{LS}(a,b) = \frac{\sigma^2 L_t L_r}{\alpha}. \tag{23}$$

2) LS FFT-Based Channel Estimator: As we mentioned earlier, the LS FFT-based channel estimator first simply chooses the L largest taps, and then replaces the $(K-L)$ remaining taps by zero. This operation can be equivalently described by using the $K \times K$ tap-selection matrix $\mathbf{T}$ given by

$$\mathbf{T} = \mathrm{diag}\{1,1,\ldots,0,1,\ldots,0\}, \tag{24}$$

where 0's and 1's represent non-selected and selected taps, respectively. There are $(K-L)$ 0's and L 1's elements in the diagonal elements of $\mathbf{T}$. By using the tap-selection matrix $\mathbf{T}$, the temporal LS FFT-based-estimate of the channel impulse response between the a^{th} receiver and b^{th} transmitter can be described by

$$\begin{aligned}\hat{\mathbf{h}}_{FFT_{ab}}(m) &= \mathbf{TG}\hat{\mathbf{H}}_{LS_{ab}}(m)\\ &= \mathbf{TGF}\mathbf{h}_{ab}(m) + \mathbf{TGZ}_{1_{ab}}(m),\end{aligned} \tag{25}$$

by plugging in $\hat{\mathbf{H}}_{LS_{ab}}(m)$ in (16).

Similarly to (21), the channel estimation error can be described by, using $\mathbf{h}_{ab}^{G}(m)$ in (20) and $\hat{\mathbf{h}}_{FFT_{ab}}(m)$ in (25),

$$\begin{aligned}\tilde{\mathbf{h}}_{FFT_{ab}}(m) &= \mathbf{h}_{ab}^{G}(m) - \hat{\mathbf{h}}_{FFT_{ab}}(m)\\ &= (\mathbf{GF} - \mathbf{TGF})\mathbf{h}_{ab}(m) - \mathbf{TGZ}_{1_{ab}}(m),\end{aligned} \tag{26}$$

Now let us define $\mathcal{W}_2 \in \{0,\ldots,K-1\}\backslash\mathcal{W}_1$ to be a set of the non-selected $(K-L)$ less significant taps, and $w_2 \in \mathcal{W}_2$ and $w_1 \in \mathcal{W}_1$ are row indices indicating the 0's and 1's elements of $\mathbf{T}$, respectively. It can be shown that

$$\begin{aligned}[\mathbf{GF} - \mathbf{TGF}]_{w_2,1:L} = \tfrac{1}{K}[&f(w_2-1)e^{j\xi(w_2-1)},\ldots,\\ &f(w_2-1-\tau_{L-1})e^{j\xi(w_2-1-\tau_{L-1})}],\end{aligned} \tag{27}$$

where $\tau_0 = 0$. Therefore, by substituting (27) into (26), we can express each part of the channel estimation error as follows,

$$\begin{aligned}&[(\mathbf{GF} - \mathbf{TGF})\mathbf{h}_{ab}(m)]_{w_1\in\mathcal{W}_1} = [\mathbf{TGZ}_{1_{ab}}(m)]_{w_2\in\mathcal{W}_2} = 0,\\ &[(\mathbf{GF} - \mathbf{TGF})\mathbf{h}_{ab}(m)]_{w_2\in\mathcal{W}_2}\\ &= \tfrac{1}{K}\textstyle\sum_{l=0}^{L-1} h_{ab}(m,l)f(w_2-1-\tau_l)e^{j\xi(w_2-1-\tau_l)},\ \text{and}\\ &[\mathbf{TGZ}_{1_{ab}}(m)]_{w_1\in\mathcal{W}_1} = [\mathbf{Z}_{1_{ab}}^{G}(m)]_{w_1\in\mathcal{W}_1}.\end{aligned} \tag{28}$$

From (28), it is readily shown that the channel estimation error of the LS FFT-based channel estimator are due to two error sources: the model mismatch error, i.e. $[(\mathbf{GF} - \mathbf{TGF})\mathbf{h}_{ab}(m)]_{w_2\in\mathcal{W}_2}$, and the corresponding noise effect, i.e. $[\mathbf{TGZ}_{1_{ab}}(m)]_{w_1\in\mathcal{W}_1}$. By substituting (28) into (26), we have the $\mathrm{MSE}_{FFT}(a,b)$ of the LS FFT-based channel estimator as

$$\begin{aligned}\mathrm{E}[\|\tilde{\mathbf{h}}_{FFT_{ab}}(m)\|^2] = \tfrac{1}{K^2}\textstyle\sum_{w_2\in\mathcal{W}_2}\sum_{l=0}^{L-1}\mathrm{E}[|h_{ab}(m,l)\\ \cdot f(w_2-1-\tau_l)|^2] + \tfrac{L\sigma^2}{K\alpha},\end{aligned} \tag{29}$$

in which the assumption that the channel and noise, and channels from different paths are mutually uncorrelated, is exploited. For L_r-receiver L_t-transmitter MIMO systems, the overall MSE_{FFT} in (29) can be expressed as follows,

$$\mathrm{MSE}_{FFT}^{T} = \frac{\chi}{K^2} + \frac{L\sigma^2 L_t L_r}{K\alpha}, \tag{30}$$

where $\frac{\chi}{K^2} = \sum_{a=1}^{L_r}\sum_{b=1}^{L_t}\sum_{j=1}^{K}\mathrm{E}[\|[\hat{\mathbf{h}}_{LS_{ab}}(m)]_j\|^2] - \eta_2 - \sum_{a=1}^{L_r}\sum_{b=1}^{L_t}\sum_{w_1\in\mathcal{W}_1}\mathrm{E}[\|[\hat{\mathbf{h}}_{LS_{ab}}(m)]_{w_1}\|^2]$ with $\eta_2 = \frac{(K-L)\sigma^2 L_t L_r}{K\alpha}$.

First, we consider the case of the multipath delay profiles with integer delays. In this case, the model mismatch error χ is equal to zero. Since $L \le K$ and by referring to (23), we can see that the channel estimation performance of the LS FFT-based channel estimator is superior to that of the PEDB-LS channel estimator in this case, i.e. $\mathrm{MSE}_{FFT}^{T} \le \mathrm{MSE}_{LS}^{T}$. Using $\chi = 0$, we have

$$\begin{aligned}&\textstyle\sum_{a=1}^{L_r}\sum_{b=1}^{L_t}\sum_{w_1\in\mathcal{W}_1}\mathrm{E}[\|[\hat{\mathbf{h}}_{LS_{ab}}(m)]_{w_1}\|^2]\\ &= \textstyle\sum_{a=1}^{L_r}\sum_{b=1}^{L_t}\sum_{j=1}^{K}\mathrm{E}[\|[\hat{\mathbf{h}}_{LS_{ab}}(m)]_j\|^2] - \frac{(K-L)\sigma^2 L_t L_r}{K\alpha}\end{aligned} \tag{31}$$

The observation in (31) indicates that in order to achieve the minimum MSE of the LS FFT-based channel estimator, the L largest taps must be capable of capturing the average total energy of channels in the presence of AWGN.

For the case of the multipath delay profiles with non-integer delays, a non-zero model mismatch error χ exists, as shown in (30), due to the leakage phenomenon. Hence, it is important to study the joint effects of the tap length L and the noise level σ^2 on the MSE measure.

V. The Proposed Adaptive LS FFT-Based Channel Estimator

In this section, we propose an adaptive LS FFT-based channel estimation approach in which the number of significant taps used in channel estimation can be adjustable in order to minimize the model mismatch error and the corresponding noise effect. The model mismatch error in the LS FFT-based channel estimation stems from the fact that a fixed number of L (or P) largest taps is used in the channel estimation process for all signal-to-noise ratio (SNR) values. In the proposed adaptive LS FFT-based approach, the number of significant taps P is chosen to achieve the intuitive goal that the average total energy of the channels dissipating in each tap is completely captured in order to compensate the model mismatch error. Specifically, the number of significant taps P_{opt} used to capture the CSI in $\hat{\mathbf{h}}_{LS_{ab}}(m)$ in (18) is obtained by solving the following optimization problem:

This full text paper was peer reviewed at the direction of IEEE Communications Society subject matter experts for publication in the WCNC 2006 proceedings.

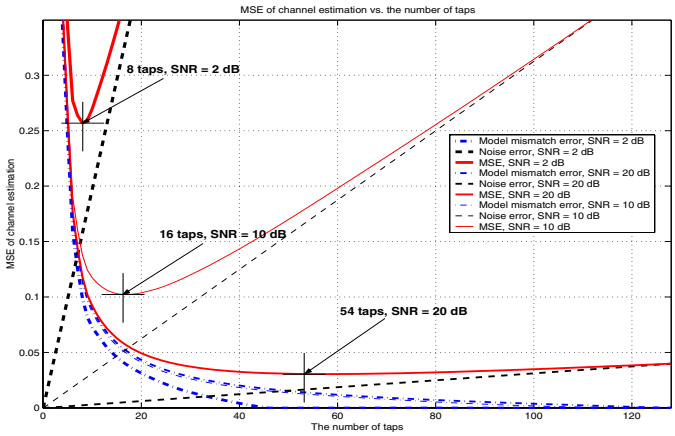

Fig. 1: Theoretical examples of the model mismatch error, the noise effect, and the overall MSE of the LS FFT-based channel estimator as a function of the number of significant taps P.

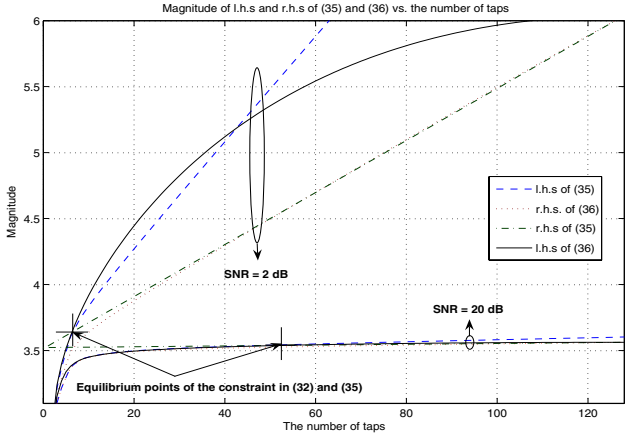

Fig. 2: The relationship between l.h.s and r.h.s of (35) and (36) based on numerical calculations.

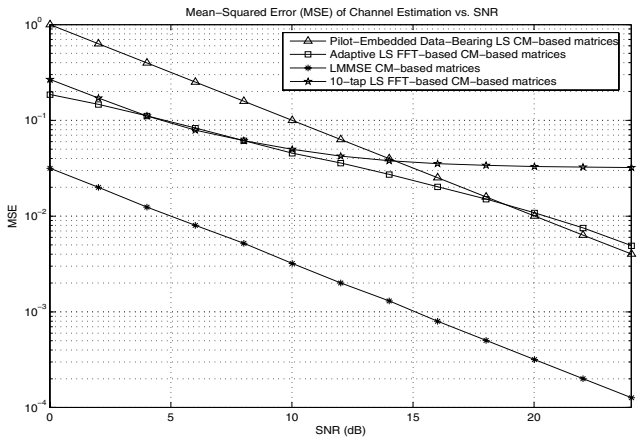

Fig. 3: The graph of MSEs of the channel estimation in quasi-static fading channels.

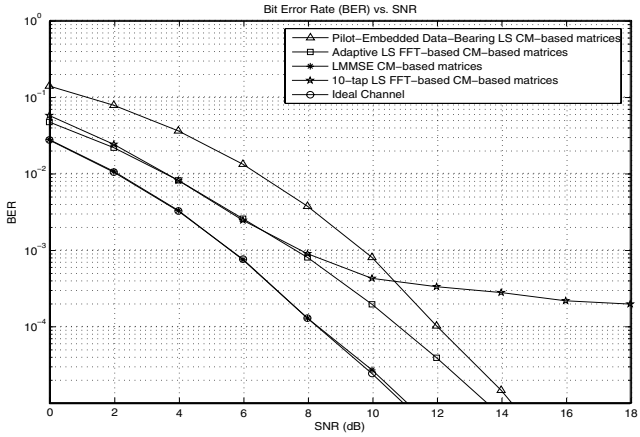

Fig. 4: The graph of BERs of the pilot-embedded SF-coded MIMO-OFDM system in quasi-static fading channels.

$$P_{opt} = \min(P) \quad \text{s.t.}$$
$$\sum_{a=1}^{L_r}\sum_{b=1}^{L_t} \mathrm{E}\left[\max_{\mathcal{W}_p,|\mathcal{W}_p|=P} \sum_{i\in\mathcal{W}_p} \|[\hat{\mathbf{h}}_{LS_{ab}}(m)]_i\|^2\right] \geq$$
$$\sum_{a=1}^{L_r}\sum_{b=1}^{L_t}\sum_{j=1}^{K} \mathrm{E}[\|[\hat{\mathbf{h}}_{LS_{ab}}(m)]_j\|^2] - \frac{(K-P)L_tL_r\sigma^2}{K\alpha}. \quad (32)$$

It is clear that, for a given P, the solution of achieving $\max_{\mathcal{W}_p,|\mathcal{W}_p|=P} \sum_{i\in\mathcal{W}_p} \|[\hat{\mathbf{h}}_{LS_{ab}}(m)]_i\|^2$ is to choose $\mathcal{W}_p$ as the indices of the P largest taps ($P = L$ in the previous sections).

Now let us intuitively explain why (32) in details. If we assume a perfect situation, then the most desired criteria used to determine the number of significant taps P is the MSE^T_{FFT} in (30), such that the optimization solution is expressed as

$$P_{opt} = \min_P \{\mathrm{MSE}^T_{FFT}(P)\}. \quad (33)$$

First, instead of minimizing $\mathrm{MSE}^T_{FFT}(P)$ directly, we want to take advantage of specific observations revealed in the two terms of (30). In Fig. 1, we plot the corresponding χ/K^2 term and the noise error term $\frac{L\sigma^2L_tL_r}{K\alpha}$ as a function of P under several SNR levels with the setting parameters described in Section VI. From this figure, we note that χ/K^2 converges to zero as P increases, meaning that more taps can be used to compensate the model mismatch error. Also, it is seen that the resulting P_{opt} increases as SNR increases. In addition it is noted that P_{opt} can be approximately determined by locating the intersection point of the curve of the model mismatch error and the curve of the noise error. Therefore, the problem in (33) can be formulated as

$$P_{opt} = \min(P) \quad \text{s.t.} \quad \{\frac{\chi}{K^2} \leq \frac{P\sigma^2L_tL_r}{K\alpha}\}. \quad (34)$$

Or equivalently, by substituting χ, we have

$$P_{opt} = \min(P) \quad \text{s.t.}$$
$$\sum_{a=1}^{L_r}\sum_{b=1}^{L_t}\sum_{i\in\mathcal{W}_p} \mathrm{E}\left[\|[\hat{\mathbf{h}}_{LS_{ab}}(m)]_i\|^2\right] + \frac{P\sigma^2L_tL_r}{K\alpha} \geq$$
$$\left(\sum_{a=1}^{L_r}\sum_{b=1}^{L_t}\sum_{j=1}^{K} \mathrm{E}[\|[\hat{\mathbf{h}}_{LS_{ab}}(m)]_j\|^2] - \frac{(K-P)L_tL_r\sigma^2}{K\alpha}\right) \quad (35)$$

However, in practice, since $\mathcal{W}_p$ is an unknown set, it is not feasible to compute the term $\sum_{a=1}^{L_r}\sum_{b=1}^{L_t}\sum_{i\in\mathcal{W}_p} \mathrm{E}\left[\|[\hat{\mathbf{h}}_{LS_{ab}}(m)]_i\|^2\right]$ directly. In stead, for each transmission, depending on the real observations, for different P, we instantaneously compute the term $\max_{\{\mathcal{W}_p,|\mathcal{W}_p|=P\}} \sum_{i\in\mathcal{W}_p} \|[\hat{\mathbf{h}}_{LS_{ab}}(m)]_i\|^2$. Then empirical expectation is calculated. Overall, we compute the following term $\sum_{a=1}^{L_r}\sum_{b=1}^{L_t} \mathrm{E}\left[\max_{W_p,|W_p|=P} \sum_{i\in W_p} \|[\hat{\mathbf{h}}_{LS_{ab}}(m)]_i\|^2\right]$.

This full text paper was peer reviewed at the direction of IEEE Communications Society subject matter experts for publication in the WCNC 2006 proceedings.

Since

$$\sum_{a=1}^{L_r}\sum_{b=1}^{L_t}\mathrm{E}\left[\max_{\mathcal{W}_p,|\mathcal{W}_p|=P}\sum_{i\in\mathcal{W}_p}\|[\hat{\mathbf{h}}_{LS_{ab}}(m)]_i\|^2\right] \geq \sum_{a=1}^{L_r}\sum_{b=1}^{L_t}\sum_{i\in\mathcal{W}_p}\mathrm{E}\left[\|[\hat{\mathbf{h}}_{LS_{ab}}(m)]_i\|^2\right], \quad (36)$$

where $\mathcal{W}_p$ is a set of the P largest taps. We note that the left hand is based on order statistics. In our case, since the components in $\hat{\mathbf{h}}_{LS_{ab}}(m)$ follow non-identical distributions, due to the complex nature of order statistics, it is infeasible to find the theoretical close-form expression of the l.h.s of (36) in term of the r.h.s of (36). Numerical examples are plotted in Fig. 2 to demonstrate the relationship between the l.h.s of (35) and the l.h.s of (36). From Fig. 2, we can see that the curves of the l.h.s of (35) and (36) are close together when the number of taps are small until the intersection point between these two curves and the r.h.s of (35) for both SNR = 2 and 20 dB. This phenomenon indicates that by replacing the l.h.s of (35) by the l.h.s of (36) for determining the minimum number of significant taps that yield the equality to the constraint of (35), the resulting number of taps are mostly the same as solving (35) directly. It is worth noticing that in the regimes beyond the intersection point, these two curves are different; however, this phenomenon does not affect the minimum number of significant taps since we never exploit their relationship in these regimes.

Based on the above observations, we propose to replace the l.h.s of (35) by the l.h.s of (36), and thus replace the inequality constraint in (35) by the inequality constraint in (32). Therefore, we have the proposed scheme in determining P_{opt} as described in (32). In this sense, we could regard the proposed scheme in (32) as a sub-optimal approach in determining P_{opt}. However, in most cases, the P_{opt} determined by solving the problem in (32) is almost identical to the optimum solution obtained by using an exhaustive search for the minimum MSE_{FFT}^{T} in (30). While the later case serves as a theoretical ideal solution.

VI. Simulation Results

Simulations are conducted under quasi-static frequency-selective Rayleigh fading channels. The simulated SF block code is obtained from Alamouti's structure as in [1], using a BPSK constellation for two transmit and two receive antennas. The COST207 typical urban (TU) six-ray normalized power delay profile [9] with delay spread of 5 μs is studied. The entire channel bandwidth, 1 MH_z, is divided into $K = 128$ subcarriers in which four subcarriers on each end are served as guard tones, and the rest (120 tones) are used to transmit data. To make the tone orthogonal to each other, the symbol duration is 128 μs, and additional 20 μs guard interval is used as the cyclic prefix length in order to protect the ISI due to the multipath delay spread. The equal block-power allocation, i.e. $\beta = \alpha = 0.5$ W, is employed, the normalized SF-coded symbol block-power is 1 W, $N = 2$, and $M = N + L_t = 4$. The CM-based structure in (8) is selected as the representative of three structures studied in [7]. In this experiment, the channel impulse response $h_{ab}(m, l)$'s in (2) are based on Jake's model [10], when $f_d * T_f = 0.08$ (fast fading) with f_d being the Doppler's shift.

In Fig.3, the MSEs of the PEDB-LS, 10-tap LS FFT-based, adaptive LS FFT-based, and LMMSE channel estimators [3], are shown. Notice that the PEDB-LS approach has a higher MSE in low SNR regimes than that of the 10-tap LS FFT-based and the adaptive LS FFT-based approaches. In high SNR regimes, the PEDB-LS and adaptive LS FFT-based approaches performs better than the 10-tap LS FFT-based one in which the error floor caused by the model mismatch error occurs, whereas the former two do not suffer from this severe error floor. It is worth noticing that the LMMSE estimator serves as the channel estimation performance bound at the price of the intensive computational complexity and the additional channel correlation information.

In Fig.4, the BER comparisons are shown. Notice that the 10-tap LS FFT-based and adaptive LS FFT-based estimation performances are quite close in low SNR regimes, whereas the PEDB-LS approach performs worse, in which the 2-dB SNR difference at BER of 10^{-3} is observed. In high SNR regimes, the 10-tap LS FFT-based estimator suffers from the error floor, say at BER of 2×10^{-4}, whereas the others do not. At BER of 10^{-4}, the SNR differences between the ideal-channel scheme, where the true channel impulse response is employed, and the adaptive LS FFT-based and PEDB-LS estimators are 2.2 dB and 3.6 dB, respectively, whereas the LMMSE estimator provides the error probability coinciding with the ideal-channel scheme.

VII. Conclusion

In this paper, we have proposed an adaptive LS FFT-based channel estimator for improving the performances of the LS FFT-based and PEDB-LS estimators, under the framework of pilot-embedded data-bearing approach for joint channel estimation and data detection. For quasi-static TU-profile fading channels, simulations show that the adaptive LS FFT-based estimator provides superior performance to that of the 10-tap LS FFT-based and PEDB-LS approaches. For instance, at BER of 10^{-4}, the SNR differences are as 2.2 dB and 3.6 dB, respectively, for the adaptive LS FFT-based and the PEDB-LS estimators compared with the ideal-channel scheme, whereas the 10-tap LS FFT-based estimator suffers from the severe error floor caused by the model mismatch error.

References

[1] Weifeng Su, Z. Safar, M. Olfat, and K.J.R. Liu, "Obtaining full-diversity space-frequency codes from space-time codes via mapping," *IEEE Trans. Signal Processing*, Vol. 51, No. 11, pp. 2905-2916, Nov. 2003.

[2] Imad Barhumi, G. Leus, and M. Moonen, "Optimal training design for MIMO-OFDM systems in mobile wireless channels," *IEEE Trans. Signal Processing*, Vol. 51, No. 6, pp. 1615-1624, June 2003.

[3] Y. Gong and K.B. Lataief, "Low complexity channel estimation for space-time coded wideband OFDM systems," *IEEE Trans. Wireless Commu.*, Vol. 2, No. 5, pp. 876-882, Sept. 2003.

[4] Y. (Geoffrey) Li, "Channel estimation for OFDM systems with trsmitter diversity in mobile wireless channels," *IEEE J. Select. Areas Commu.*, Vol. 17, No. 3, pp. 461-471, Mar. 1999.

[5] J. J. van de Beek, O. Edfors, M. Sandell, S. K. Wilson, and P. O. Borjesson, "On channel estimation in OFDM systems," *Proc. 45th IEEE VTC*, Chicago, IL, pp. 815-819, July 1999.

[6] X. Wang and K.J.R. Liu, "Model based channel estimation framework for MIMO multicarrier communication systems," *IEEE Trans. Wireless Commu.*, Vol. 4, No. 3, pp. 1-14, May 2005.

[7] C. Pirak, Z.J. Wang, K.J.R. Liu, and S. Jitapunkul, "Performance analysis for pilot-embedded data-bearing approach in space-time coded MIMO systems," *Proc. IEEE ICASSP*, Philadelphia, PA, pp.593-596, Mar. 2005.

[8] A.V. Geramita and J. Seberry, *Orthogonal Designs*, Marcel Dekker, INC., NY, 1979.

[9] G. Stuber, *Principles of Mobile Communications*, Kluwer, MA, 2001.

[10] W.C. Jakes, Jr., "Multipath Interference", *Microwave Mobile Communication* W.C. Jakes, Jr., Ed., Wiley, NY, 1974, pp. 67-68.

This full text paper was peer reviewed at the direction of IEEE Communications Society subject matter experts for publication in the WCNC 2006 proceedings.